AD-A145 822 INFERENCE OF EQUATORIAL FIELD-LINE INTEGRATED ELECTRON DENSITY VALUES USING WHISTLERS(U) AIR FORCE GEOPHYSICS LAB HANSCOM AFB MA D ANDERSON ET AL. 01 AUG 84 1/1

UNCLASSIFIED AFGL-TR-84-0195 F/G 4/1 NL

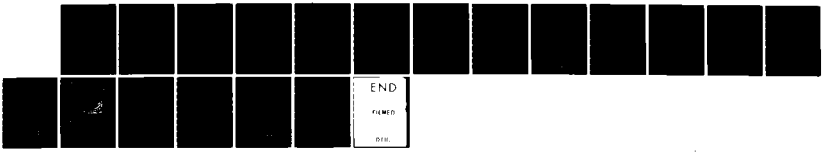

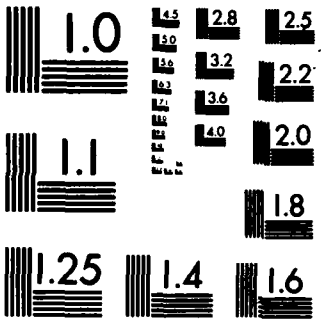

AD-A145 822

UNCLASSIFIED

SECURITY CLASSIFICATION OF THIS PAGE

REPORT DOCUMENTATION PAGE

1a. REPORT SECURITY CLASSIFICATION: UNCLASSIFIED	1b. RESTRICTIVE MARKINGS: N/A
2a. SECURITY CLASSIFICATION AUTHORITY: N/A	3. DISTRIBUTION/AVAILABILITY OF REPORT: Approved for public release; Distribution unlimited.
2b. DECLASSIFICATION/DOWNGRADING SCHEDULE: N/A	
4. PERFORMING ORGANIZATION REPORT NUMBER(S): AFGL-TR-84-0195	5. MONITORING ORGANIZATION REPORT NUMBER(S)
6a. NAME OF PERFORMING ORGANIZATION: Air Force Geophysics Laboratory; 6b. OFFICE SYMBOL (If applicable): LIS	7a. NAME OF MONITORING ORGANIZATION
6c. ADDRESS (City, State and ZIP Code): Hanscom AFB, MA 01731	7b. ADDRESS (City, State and ZIP Code)
8a. NAME OF FUNDING/SPONSORING ORGANIZATION: Air Force Geophysics Laboratory; 8b. OFFICE SYMBOL (If applicable): LIS	9. PROCUREMENT INSTRUMENT IDENTIFICATION NUMBER
8c. ADDRESS (City, State and ZIP Code): Hanscom AFB, MA 01731	10. SOURCE OF FUNDING NOS.

PROGRAM ELEMENT NO.	PROJECT NO.	TASK NO.	WORK UNIT NO.
61102F	2310	G9	01

11. TITLE (Include Security Classification): Inference of equatorial field-line integrated electron density values Using Whistlers

12. PERSONAL AUTHOR(S): D. Anderson, P.M. Kintner* and M.C. Kelley*

13a. TYPE OF REPORT	13b. TIME COVERED	14. DATE OF REPORT (Yr., Mo., Day)	15. PAGE COUNT
REPRINT	FROM _____ TO _____	1984 August 1	17

16. SUPPLEMENTARY NOTATION: *Cornell University, School of Electrical Engineering, Ithaca, NY
Reprinted from Proceedings of the 7th International Symposium on Equatorial Aeronomy, 22-29 March 1984, Hong Kong (Editor: G. O. Walker)

17. COSATI CODES		
FIELD	GROUP	SUB. GR.

18. SUBJECT TERMS (Continue on reverse if necessary and identify by block number): Electron density, whistlers, low latitude ionosphere

19. ABSTRACT (Continue on reverse if necessary and identify by block number)

The nighttime electron density integrated along a magnetic field line at very small L-values ~~(L = 1.06)~~ is inferred by comparing whistler dispersions measured from a sounding rocket with model ionospheric calculations. At a local time of 0500 LT, the electron density of the F-layer valley was found to be about $1 \times 10^3/cm^3$. We suggest that this technique can be applied to earlier times in the local evening to determine ionospheric conditions which benefit the growth of low latitude plasma instabilities.

DTIC FILE COPY

1000/cc

DTIC ELECTE SEP 16 1984

20. DISTRIBUTION/AVAILABILITY OF ABSTRACT	21. ABSTRACT SECURITY CLASSIFICATION
UNCLASSIFIED/UNLIMITED ☒ SAME AS RPT. ☐ DTIC USERS ☐	UNCLASSIFIED

22a. NAME OF RESPONSIBLE INDIVIDUAL	22b. TELEPHONE NUMBER (Include Area Code)	22c. OFFICE SYMBOL
David N. Anderson	617-861-3220	AFGL/LIS

DD FORM 1473, 83 APR — EDITION OF 1 JAN 73 IS OBSOLETE.

Unclassified

SECURITY CLASSIFICATION OF THIS PAGE

AFGL-TR-84-0195

Inference of Equatorial Field-Line-Integrated Electron Density Values Using Whistlers

D. Anderson [1]
Air Force Geophysics Lab., Hanscom Air Force Base, MA 01731

P. M. Kintner and M. C. Kelley
School of Electrical Engineering, Cornell University, Ithaca, NY 14853

Abstract. The nighttime electron density integrated along a magnetic field line at very small L-values (L ≈ 1.06) is inferred by comparing whistler dispersions measured from a sounding rocket with model ionospheric calculations. At a local time of 0500 LT, the electron density in the F-layer valley was found to be about 1 x $10^3/cm^3$. We suggest that this technique can be applied to earlier times in the local evening to determine ionospheric conditions which benefit the growth of low latitude plasma instabilities.

Introduction

During the post sunset period the equatorial ionosphere is known to be turbulent over scale sizes from tens of kilometers to tens of centimeters. The turbulence (equatorial spread-F) is believed to originate at long wavelengths through an interchange process, such as the Rayleigh-Taylor instability or the ExB drift instability. In brief, a plasma depletion develops at the bottom of the F-layer which rises like a bubble through the F-region. Many of the long wavelength properties can be simulated using two dimensional models (Ossakow, 1981) which neglect variations along the field line. Nonetheless, the process is known to be three dimensional. ALTAIR radar measurements show dramatically that the plasma depletions fully extend along magnetic lines (Tsunoda, 1980). In addition, the field line integrated parameters such as Pedersen conductivity and electron content are important in determining the instability growth rates

(Anderson and Haerendel, 1979). On the other hand, it is very difficult to measure the electron density below the dense F-region. In this paper we apply an old technique (measuring whistler dispersion) to validate model calculations of equatorial field line integrated electron densities. We also suggest that measuring whistler dispersion at appropriate local times may be useful in determining whether or not ambient ionospheric conditions exist which benefit the growth of low latitude plasma instabilities.

VLF waves below the electron gyrofrequency propagate dispersively. For conditions at the equatorial ionosphere the local dispersion is proportional to the square root of electron density and the total dispersion is proportional to the integrated square root of electron density along the group path. Our approach will be to compare observed whistler dispersion characteristics to three dimensional models of the equatorial ionosphere (Anderson, 1981) and to show that we not only can verify the model but can additionally determine the electron density within the F-layer valley. Unfortunately the local time of these particular measurements is at 0500 LT which limits their importance to spread-F theories. However the technique does not appear to be sensitive to local time and it could easily be applied in the post sunset period.

Experiment Description

A Taurus-Tomahawk sounding rocket (34.010) was launched from Punta Lobos, Peru on March 21, 1983 at 9:53:30 UT to a maximum altitude of 427 km. Its primary mission was to study the critical velocity effect using a barium shaped charge. In addition to the chemical release the payload contained a VLF electric field experiment which sensed potential fluctuations between two spheres separated by 3 meters. The launch point was about 20 km south of the magnetic dip equator and the payload traveled to the west. To a good

approximation the payload was close to the dip equator during the entire flight.

A sketch of the relation between the payload and the equatorial magnetic field is shown in Figure 1. The payload is approximately centered along the field line intersecting the payload. Now suppose that a lightning stroke occurs at one end of the field line which initiates a whistler. If we make the important assumption that the whistler propagates parallel to the magnetic field, then we expect the rocket to see a series of whistlers, each with progressively more dispersion. The first whistler trace will have dispersion associated with the square root of electron density integrated along 1/2 of the field line, the second trace will be associated with 3/2 of a field line, the third trace will be associated with 5/2 of a field line, etc. We should emphasize that there is no a priori reason to expect whistler propagation parallel to the magnetic field but the observation of a multiple hop whistler showing dispersion with the ratios 1/2, 3/2, 5/2, etc. would be strong evidence in favor of parallel or ducted propagation. The propagation of low latitude whistlers has been reviewed by Hayakawa and Tanka (1978) who concluded that multiple-hop whistler trains are rarely observed from ground stations for nighttime low latitude conditions although they may be more commonly seen from in situ observations.

An example of one of nine multiple-hop whistlers observed during the 10 minute flight is shown in Figure 2. This example occurred at 385 km altitude during the upleg. The whistler clearly shows five traces and a sixth is observable in the raw data. The dispersions for the first five traces are 4.8, 16, 30, 37, 54 $sec^{1/2}$ which nearly matches the expected ratio 1/2, 3/2, 5/2, 7/2, 9/2. The dispersion along the field line may be calculated by dividing the expected ratio into the observed dispersion and then averaging. The result

for the dispersion along one full length of the field line is 10.8 $sec^{1/2}$. This procedure has been applied to 8 other multiple hop whistlers and the estimated dispersions are shown in Figure 5 as x's. At 425 km altitude, corresponding to L = 1.066, the typical dispersion is 11 $sec^{1/2}$. This value agrees quite well with ground station observations during the 0000-0700 LT period (Hayakawa and Tanaka, 1978).

For path lengths greater than 1/2, the whistler trace in Figure 2 has a missing band between 325 Hz and 425 Hz. We believe that the missing band was caused by attenuation near the two ion crossover frequency (Smith and Brice, 1964) for a mixture of H^+ and O^+ or heavier ions. The two ion crossover frequency is given by $f_x = f_{CH^+}(N_{O^+}/N + N_{H^+}/16N)$ for O^+ where $N_{O^+} + N_{H^+} = N$. Since we expect that $N_{H^+} << N_{O^+}$, the second term can be neglected and $f_x = N_{O^+}/Nf_{CH^+}$. The H^+ cyclotron frequency at 425 km altitude on the dip equator is 340 Hz. This sets the low frequency boundary of the missing band and suggests that the local H^+ plasma density is about 5% of the total density. As the whistler propagates downward and away from the dip equator, the crossover frequency increases until the whistler reaches the foot of the field line. The H^+ cyclotron frequency at the foot of the field line (125 km altitude) is 451 Hz which also suggests an H^+ contribution to the total density of about 5%.

Model Calculations

The measured whistler dispersion yields an electron density averaged along the propagation path. To interpret this result we have employed an ionospheric model. To calculate electron densities as a function of altitude, latitude and local time, the time-dependent ion (O^+) continuity equation is solved numerically. This equation is given by

$$\frac{\partial N_i}{\partial t} + \nabla \cdot (N_i \bar{V}_i) = P_i - L_i \qquad (1)$$

where N_i ($\approx N_e$) is the ion density; P_i, the ion production rate; L_i, the ion loss rate; and V_i, the ion transport velocity. Solving equation (1) at low latitudes necessitates transforming the independent coordiates r, θ and ϕ to a coordiate system parallel and perpendicular to $\underline{B}$ (Anderson, 1973a,b). The set of coefficients for the ion continuity equation is obtained from models of the neutral composition, ion and electron temperatures and production, loss and diffusion rates as well as $\underline{E} \times \underline{B}$ drift and neutral winds. Briefly, the models are as follows:

1) The MSIS neutral atmospheric model (Hedin et al., 1977) is used to calculate N_2, O_2, and O densities and the neutral temperature as a function of altitude, latitude and local time.

2) Production, loss and diffusion rates are similar to those used by Anderson (1973b). For the photoionization coefficient at the top of the atmosphere, P_∞, a value of $6.0 \times 10^{-7} sec^{-1}$ is chosen to represent March 20-21, 1983 conditions. Electron and ion temperatures are obtained from equinox, moderate solar activity measurements at Jicamarca (March, 1969).

3) Inclusion of the vertical $\underline{E} \times \underline{B}$ drift velocity first observed by Woodman (1970) and studied in detail by Fejer et al. (1979) is essential in producing and maintaining electron density distributions observed near the magnetic equator. Figure 3 displays an $\underline{E} \times \underline{B}$ drift model appropriate for solar maximum conditions. For the March 20-21 simulation the vertical drift velocity pictured in Figure 3 was multiplied by 0.8 between 1600-2000 LT and by 1.25 between 0200-0500 LT.

4) The assumed meridional component of the neutral wind, taken from Anderson and Klobuchar (1983) is poleward during the day, reaches a maximum velocity of 70 m/sec at 1700 LT at $\pm$ 45° lat. and is symmetric about the geographic equator. The wind becomes equatorward at 1915 LT and reaches a

maximum velocity of 85 m/sec at 2300 LT. The zonal wind component is neglected because the magnetic field declination is small at Jicamarca longitudes.

Calculated electron density values as a function of altitude at the magnetic equator are illustrated in Figure 4 and compared to ground observations. In the early morning (0200 LT) the Jicamarca radar observatory made a series of density measurements as a function of altitude which showed the F-region peak at about 350 km altitude compared to the model prediction of 300 km. Nonetheless the overall profile and absolute values agree well with the model. At 0500 LT, the time of the sounding rocket flight, the only ionospheric electron density measurement available was the value of f_oF_2 from Huancayo. The altitude of f_oF_2 was 270 km in agreement with the model while the model electron density was slightly smaller than the ionosonde measurements. On board the payload was a Langmuir probe sensitive to the relative electron density; it indicated that f_oF_2 was between 240 km and 260 km. The electron density model at 0500 LT is used in the calculations that follow.

The time-dependent continuity equation is solved numerically along a number of geomagnetic field lines in order to calculate electron densities up to an altitude of 1000 km over the magnetic equator. At each point on the field line where electron density is calculated we also calculate the local plasma frequency, f_p, given by $\sqrt{80.5 \times N_e(el/m^3)}$; f_e, the electron gyrofrequency, and the whistler group velocity given by

$$V_g = \frac{c}{n_g} = \frac{c\sqrt{f}\,(f_e - f)^{3/2}}{f_p f_e}$$

where c is the speed of light. To find the period, T, for a whistler wave to travel from one end of the field line to the other, the quantity $ds/V_g(s)$ is

integrated along the field line from 125 km altitude in the northern hemisphere to 125 km altitude in the southern.

$$T = \int \frac{ds}{V_g(s)} = \frac{1}{\sqrt{f}} \int \frac{f_p f_e}{c(f_e - f)^{3/2}} ds$$

$$\text{or } \sqrt{f}\, T = D = \frac{1}{c} \int \frac{f_p}{\sqrt{f_e}} ds \quad \text{assuming that } f_e >> f.$$

D is called Disperison in units ($sec^{1/2}$).

The calculated dispersion is compared with the observed dispersion in Figure 5. We assume two different values for the electron density in the F-layer valley 1 x 10^3 el/cm^3 and 2 x 10^4 el/cm^3 which produce two different curves for the dispersion as a function of rocket altitude. The assumption of an F-layer valley electron density of 1 x 10^3 el/cm^3 produces values which agree well with observed dispersions. There is a suggestion from the data above 350 km that a slightly smaller value (20 %) of electron density in the F-layer valley would be appropriate.

Conclusions

Using whistler dispersion measurements we have verified an ionospheric model of electron density at 0500 LT and set the value of electron density within the F-layer valley to be slightly smaller than 1 x $10^3/cm^3$ for magnetic field lines which intersect the equator at higher altitudes. The results are consistent with other in situ measurements which imply electron densities in the F-layer valley at the magnetic equator of the order 10^3 at earlier local times. (McClure et al., 1977; Morse et al., 1977, Marcisi and Szuszczewicz, 1981).

At earlier local times (1900-2300) there are indications that the electron density at F-region valley altitudes (180-~~250~~ 250 km) can be as high as 2 - 3 x

10^4el/cm^3. These density values were measured in-situ by rocket-borne disc probes and a Bennett ion mass spectrometer during the Brazilian Ionospheric Modification Experiment (BIME) conducted at Natal, Brazil in September, 1982 (Narcisi and Haerendel, 1983). When these measured valley densities were included in flux-tube integrated Pedersen conductivity and electron content calculations, it was found that there was a significant increase in instability growth times, suggesting that the lack of observed, naturally-occurring equatorial plasmas depletions may be related to the relatively high electron densities within the valley region (Anderson, 1983).

To determine whether or not whistler observations might be a way of "remotely" sensing the electron density values within the valley region during the 1900 to 2300 LT period, we have calculated dispersion values as a function of altitude at the magnetic equator at 2000 LT instead of 0500 LT. The same two valley electron density values were chosen, 1 x 10^3el/cm^3 and 2 x 10^4el/cm^3, and the same input parameters discussed above were incorporated. Figure 6 presents the calculated dispersion profiles for these two cases as well as the calculated electron density profile at the magnetic equator. The post-sunset enhancement in upward ExB drift is responsible for lifting the F layer so that the valley region at the equator is below 350 km at this local time.

At the bottom of the F-layer (350 km) the difference in dispersion is appreciable. Assuming a valley density of 1 x 10^3el/cm^3 gives rise to a dispersion of 2 sec$^{1/2}$ while an assumed value of 2 x 10^4el/cm^3 yields a dispersion of 6.4 sec$^{1/2}$, with increasing altitude the dispersion values increase because both the electron density and the length of the geomagnetic field line are increasing. The difference between the two dispersion values, however, decreases because the valley densities contribute less and less to the

total field line-integrated density. It appears therefore, that a rocket launch near the magnetic equator in the post-sunset time period measuring both VLF waves and in-situ electron densities would be able to determine "remotely" valley densities associated with the field lines it is intersecting. Such a capability would help establish instability growth-rates and determine whether in fact high valley densities are a detriment to equatorial bubble formation.

Acknowledgements

We gratefully acknowledge discussions with D. Carpenter and G. Haerendel. This research was supported by NASA Grant NAG5-601 and ONR contract N00014-81-K-0018 at Cornell, and by AFOSR contract ——— .

References

Anderson, D. N., A theoretical study of the ionospheric F-region equatorial anomaly - I. Theory, Planet. Space Sci., 21, 409, 1973a.

Anderson, D. N., A theoretical study of the ionospheric F-region equatorial anomaly - II. Results in the American and Asian Sectors, Planet. Space Sci., 21, 421, 1973b.

Anderson, D. N. and G. Haerendel, The motion of depleted plasma regions in the equatorial ionosphere, 84, 4251, 1979.

Anderson, D. N., Modeling the ambient, low latitude F-region ionosphere - a review, J. Atmos. Terr. Phys., 43, 753, 1981.

Anderson, D. N., Modelling the ambient ionosphere at the time of the BIME and coloured bubbles releases, in Proceedings of the 3-5 March 1983 BIME/Coloured Bubbles Preliminary Data Review Meeting, eds. Narcisi and Haerendel, April 1983.

Anderson, D. N. and J. A. Klobuchar, Modeling the total electron content observations above Ascension Island, 88, 8020, 1983.

Fejer, B. G., D. T. Farley, R. F. Woodman, and C. Calderon, Dependence of equatorial F-region vertical drifts on season and solar cycle, J. Geophys. Res., 84, 5792, 1979.

Hayakawa, Masaki and Yoshihito Tanaka, On the propagation of low-latitude whistlers, Rev. Geophys. Space Phys., 16, 111, 1978.

Hedin, A. E., C. A. Reber, G. P. Newton, N. W. Spencer, H. C. Brinton, H. G. Mayor and W. E. Potter, A global thermospheric model based on mass spectrometer and incoherent scatter data, MSIS, J. Geophys. Res 82, 2148, 1977.

McClure, J. P., W. B. Hanson, and J. H. Hoffman, Plasma bub r and irregularities in the equatorial ionosphere, J. Geophys. Res., 82, 2650, 1977.

Morse, F. A., B. C. Edgar, H. C. Koons, C. J. Rice, W. J. Heikkila, J. H. Hoffman, B. A. Tinsley, J. D. Winningham, A. B. Christensen, R. F. Woodman, J. Pomalaza, and N. R. Teixeira, Equion, an equatorial ionospheric irregularity experiment, J. Geophys. Res., 82, 578, 1977.

Narcisi, R. S. and E. P. Szuszczewicz, Direct measurements of electron density, temperature, and ion composition in an equatorial spread-F ionosphere, J. Atmos. Terr. Phys., 43, 463, 1981.

Ossakow, S., Spread-F, A review, J. Atmos. Terr. Phys., 43, 437, 1981.

Smith, R. L. and N. Brice, Propagation in multicomponent plasmas, J. Geophys. Res., 69, 5029, 1964.

Tsunoda, R. T., Magnetic-field-aligned characteristics of plasma bubbles in the nighttime equatorial ionosphere, J. Atmos. Terr. Phys., 42, 743, 1980.

Woodman, R. F., Vertical drift velocities and east-west electric fields at the

magnetic equator, J. Geophys. Res., 75, 6249, 1970.

Figure Captions

Figure 1. A schematic diagram showing the relation between the sounding rocket payload and a whistler propagating parallel to the magnetic field. The payload would observe whistler dispersions associated with 1/2, 3/2, 5/2,...of a full magnetic field line length.

Figure 2. An example of one of nine multiple-hop whistlers observed by the sounding rocket payload 34.010.

Figure 3. Vertical ionospheric drift velocities at the magnetic equator as a function of local time.

Figure 4. The model ionospheric electron densities are compared to JRO measurements at 0200 LT and to Huancayo f_0F_2 measurements at 0500 LT.

Figure 5. The calculated dispersion for the model ionosphere using two assumed values for the F layer valley ($2 \times 10^4/cm^3$ and $1 \times 10^3/cm^3$) compared to the dispersions measured on the sounding rocket payload 34.010.

Figure 6. Calculated whistler dispersion profiles for equatorial ionospheric conditions typical of 2000 LT assuming two different values for the F-layer valley electron density ($1 \times 10^3/cm^3$ and $2 \times 10^4/cm^3$).

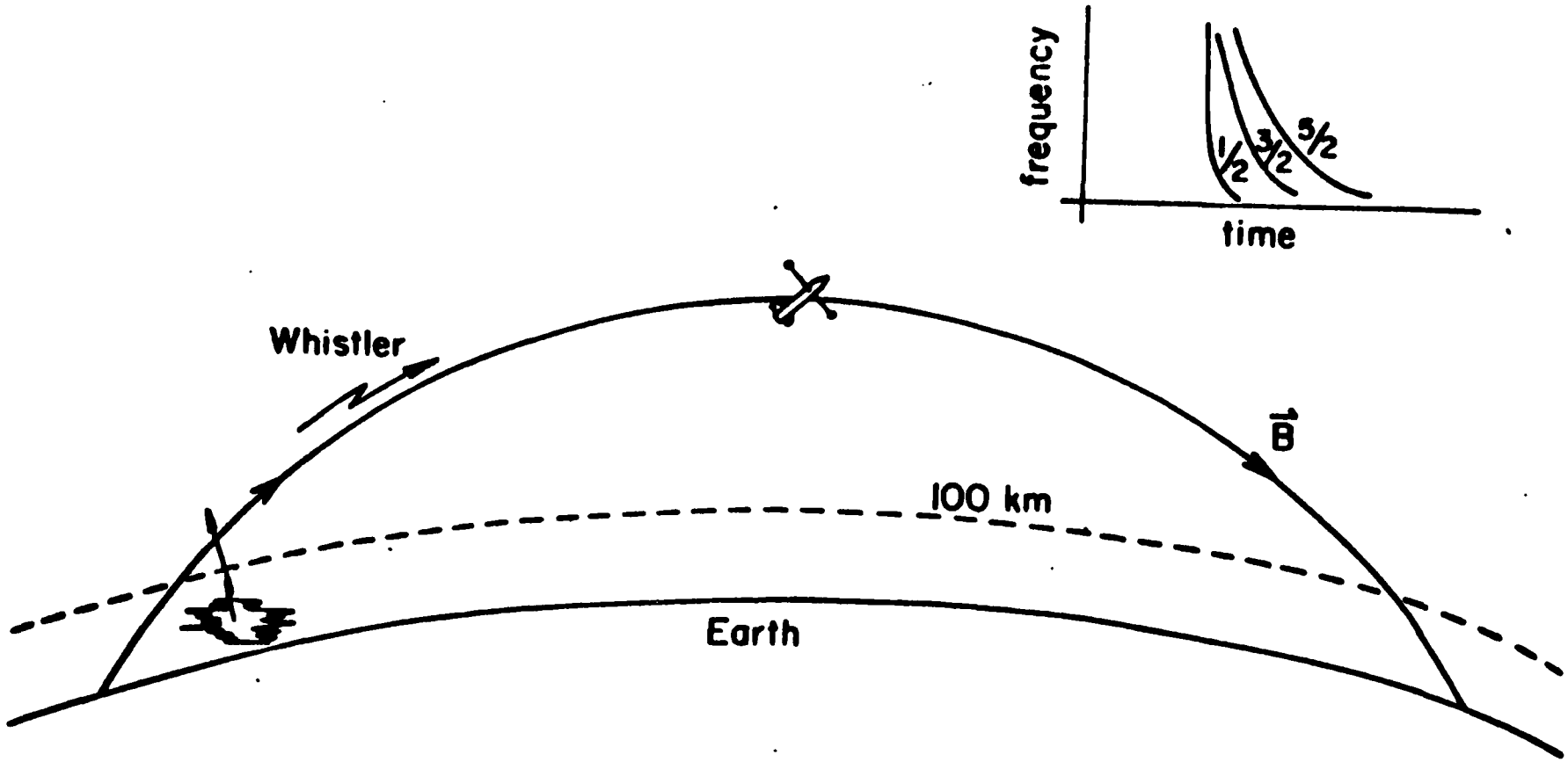

Figure 1

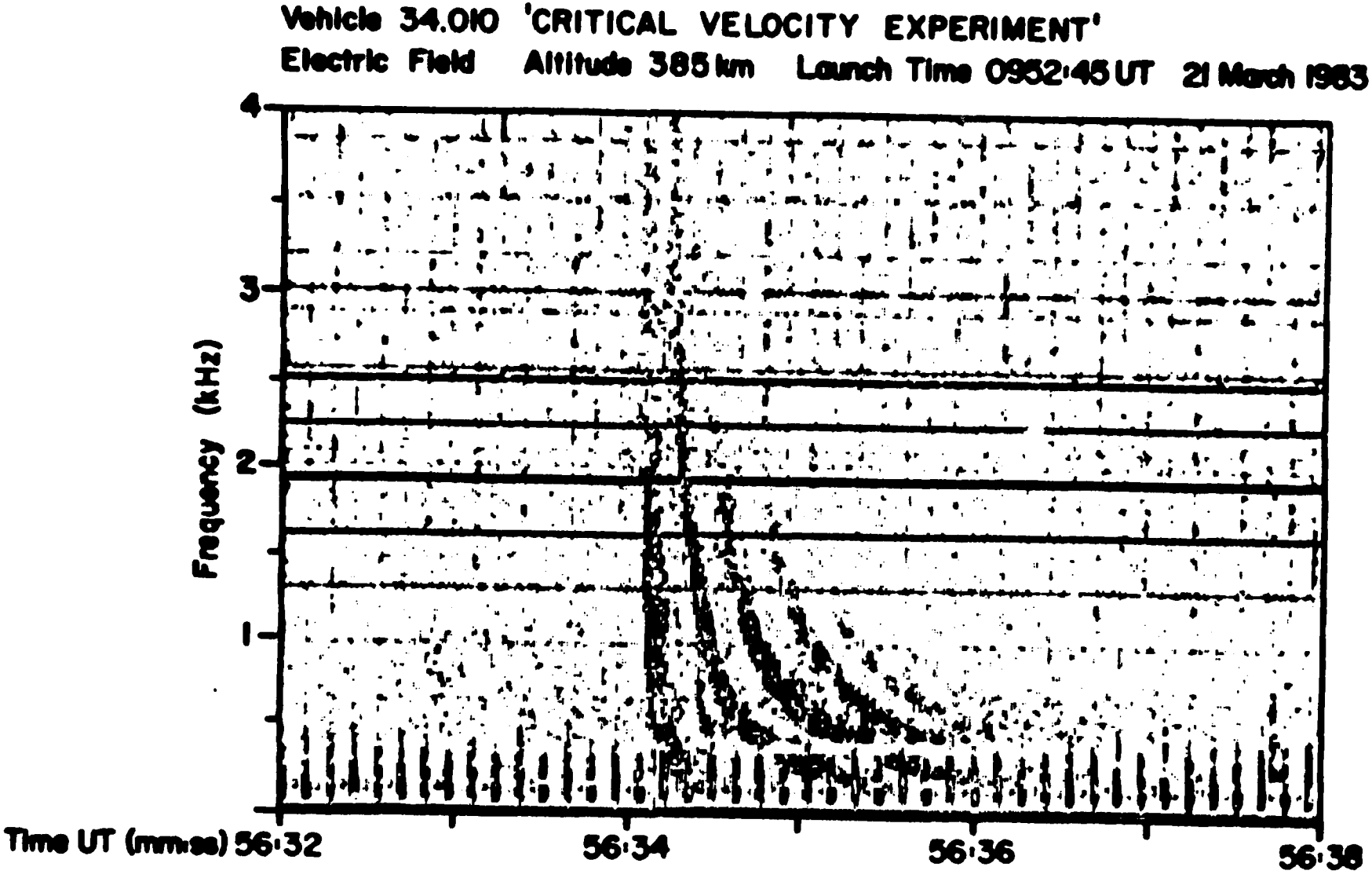
Vehicle 34.010 'CRITICAL VELOCITY EXPERIMENT'
Electric Field Altitude 385 km Launch Time 0952:45 UT 21 March 1983
Frequency (kHz)
4
3
2
1
Time UT (mm:ss) 56:32
56:34
56:36
56:38

Figure 2

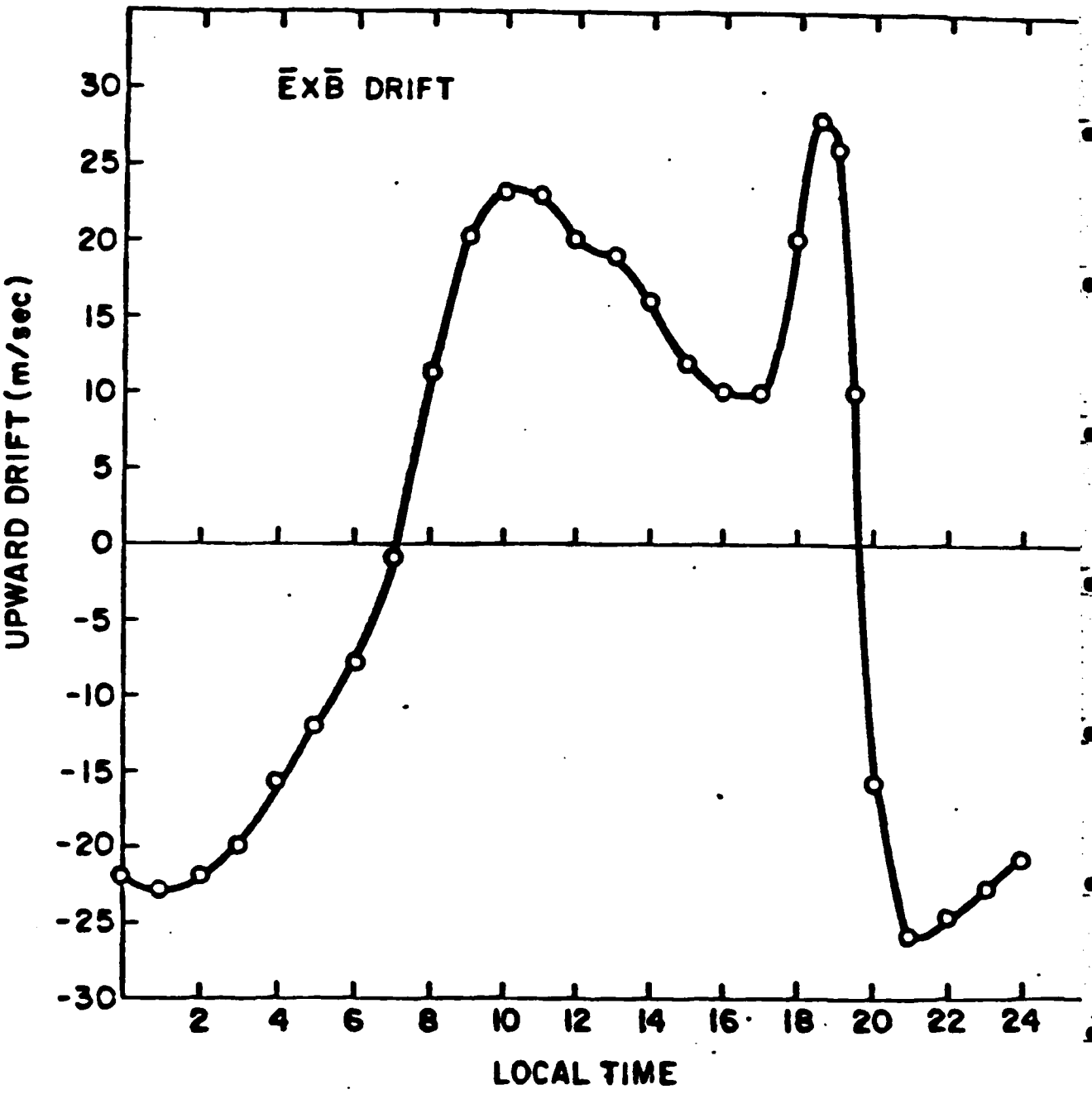
ĒXB̄ DRIFT
UPWARD DRIFT (m/sec)
30
25
20
15
10
5
0
-5
-10
-15
-20
-25
-30
2
4
6
8
10
12
14
16
18
20
22
24
LOCAL TIME

Figure 3

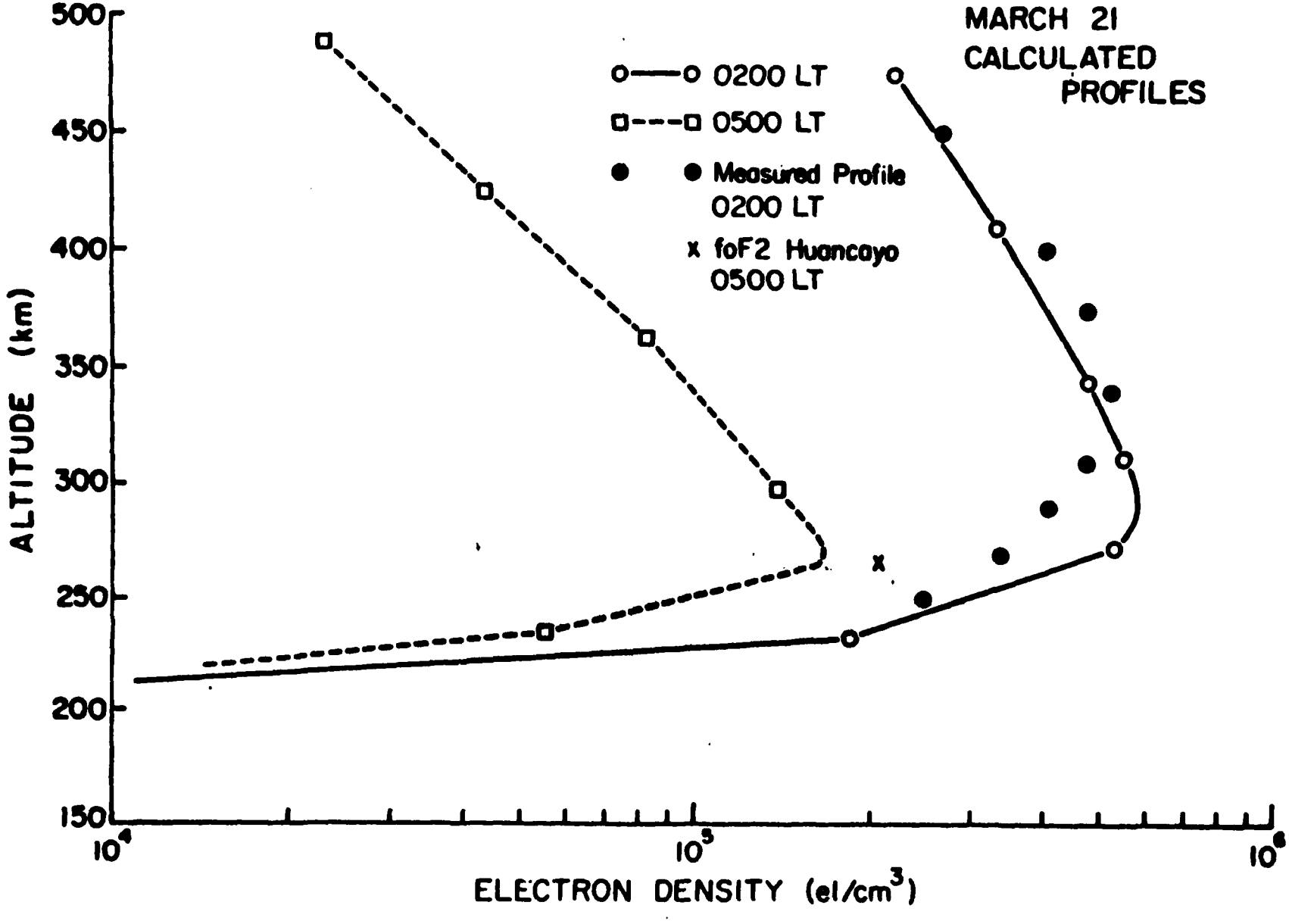
MARCH 21
CALCULATED
PROFILES
0200 LT
0500 LT
Measured Profile
0200 LT
foF2 Huancayo
0500 LT
ALTITUDE (km)
500
450
400
350
300
250
200
150
10^4
10^5
10^6
ELECTRON DENSITY (el/cm^3)

Figure 4

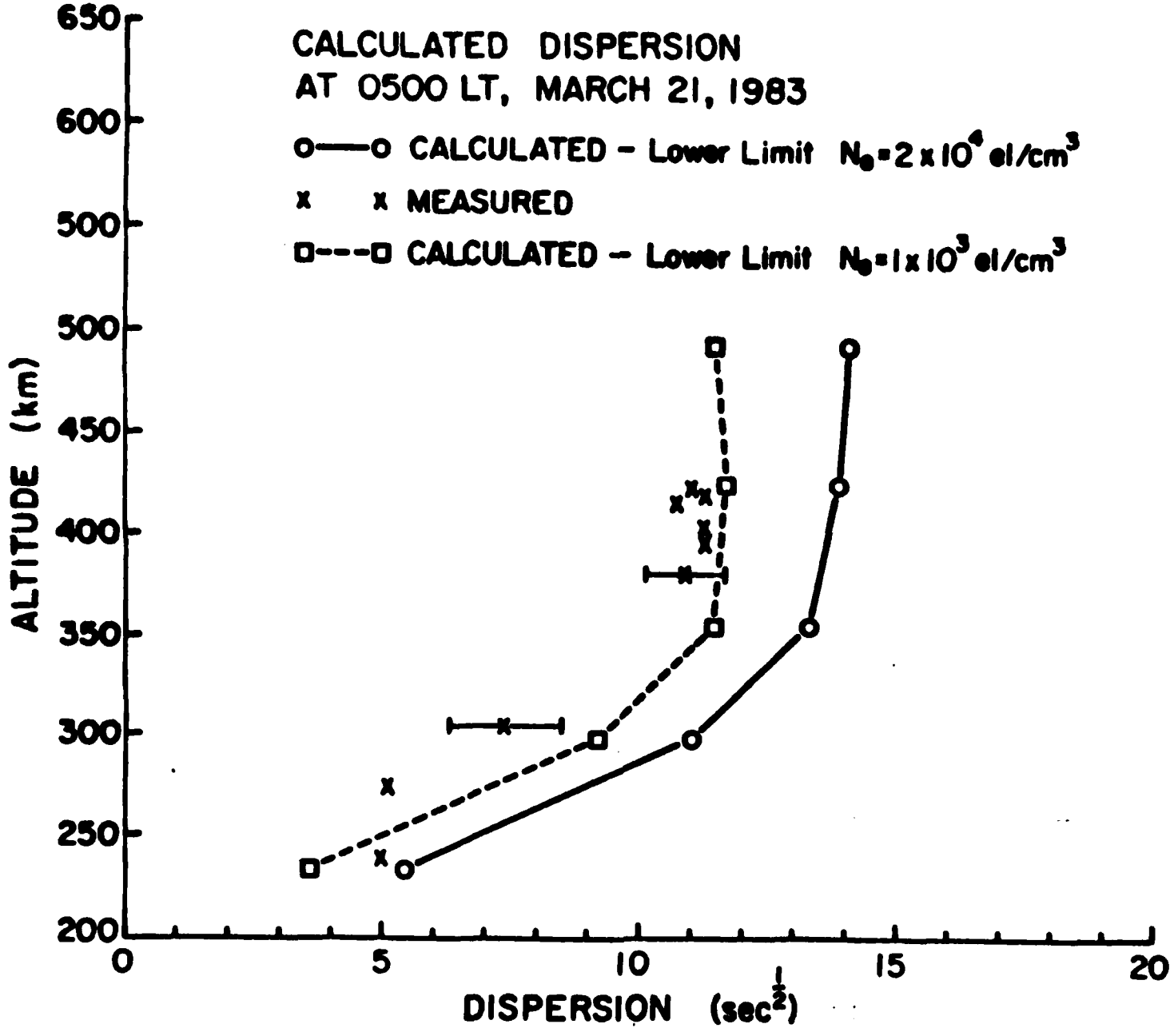
CALCULATED DISPERSION
AT 0500 LT, MARCH 21, 1983
o—o CALCULATED - Lower Limit $N_e = 2 \times 10^4$ el/cm^3
x x MEASURED
□---□ CALCULATED - Lower Limit $N_e = 1 \times 10^3$ el/cm^3
ALTITUDE (km)
650
600
500
500
450
400
350
300
250
200
0
5
10
15
20
DISPERSION (sec$^{\frac{1}{2}}$)

Figure 5

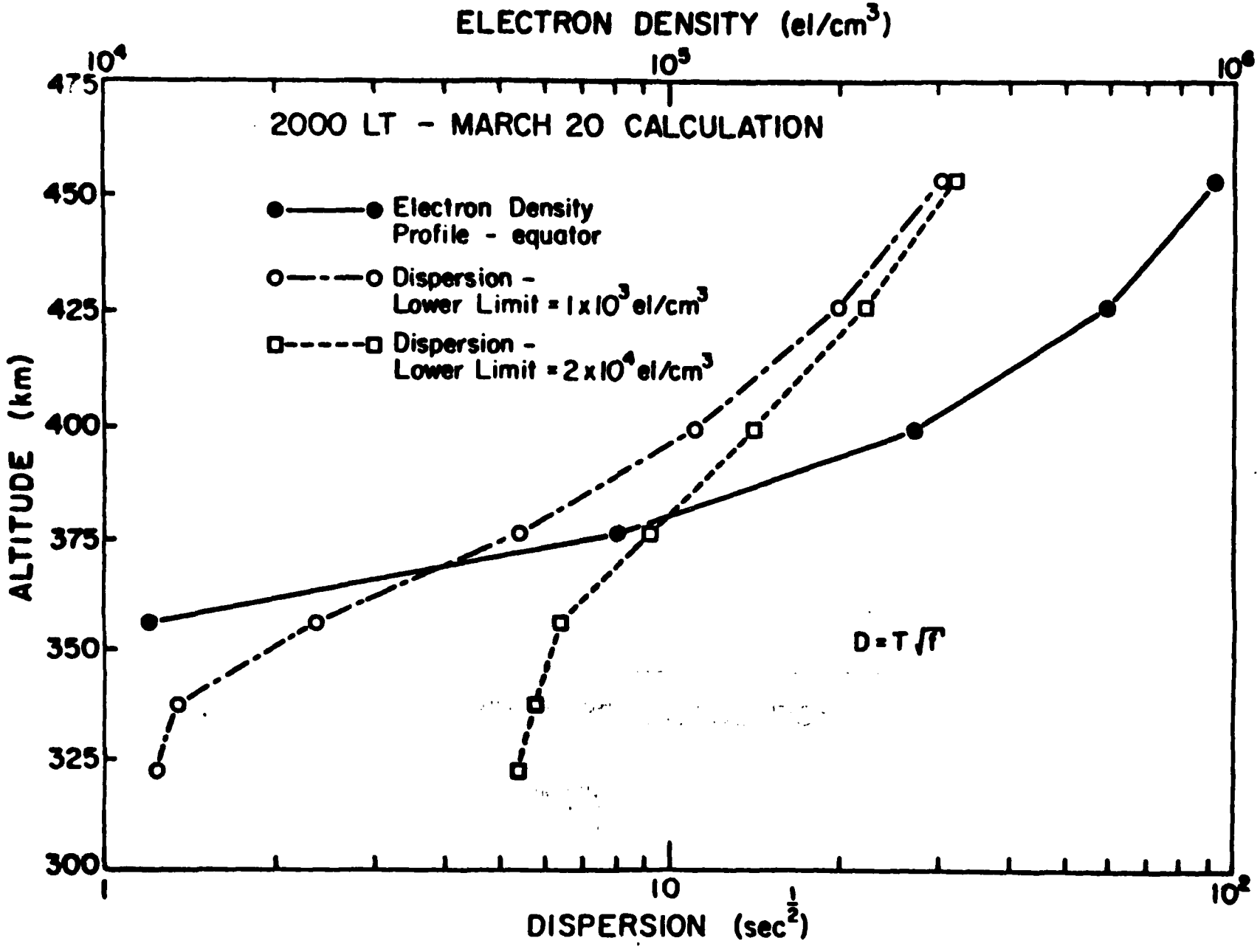
ELECTRON DENSITY (el/cm³)
10⁴
10⁵
10⁶
2000 LT - MARCH 20 CALCULATION
Electron Density Profile - equator
Dispersion - Lower Limit = 1x10³ el/cm³
Dispersion - Lower Limit = 2x10⁴ el/cm³
D = T √f
ALTITUDE (km)
475
450
425
400
375
350
325
300
1
10
10²
DISPERSION (sec^½)

Figure 6

$$\frac{\partial N_i}{\partial t} + \nabla \cdot (N_i \bar{V}_i) = P_i - L_i \qquad (1)$$

END

FILMED

10-84

DTIC